Journal of Cellular Biochemistry 81:621–638 (2001)

Ras-Induced Colony Formation and Anchorage-Independent Growth Inhibited by Elevated Expression of Purα in NIH3T3 Cells

Sharon M. Barr and Edward M. Johnson*

Departments of Pathology, Biochemistry and Molecular Biology, Mount Sinai School of Medicine, New York, 10029

Abstract Levels of Purα, a conserved, sequence-specific single-stranded DNA and RNA binding protein, fluctuate during the cell cycle, declining at the onset of S-phase and peaking at mitosis. In early G1 Purα is associated with the hypophosphorylated form of the retinoblastoma protein, Rb. Microinjection of purified Purα into NIH3T3 cells arrests the cell cycle at either G1/S or G2/M checkpoints with distinct morphological consequences. Here we ask whether expression of Purα can affect colony formation and anchorage-independent growth in *ras*-transformed NIH3T3 cells. Two to five-fold elevated levels of Purα in stably-transfected cell lines retard entry into and progression through S phase in both *ras*-transformed and non-transformed cells. Purα significantly inhibits colony formation by *ras*-transformed cells but not by non-transformed cells. In addition, cells transfected to express Purα formed only about 1/5 the number of large colonies in soft agar as control-transfected cells, demonstrating a marked inhibition of anchorage-independent growth by Purα. Biochemical analysis of nuclear and cytoplasmic Purα proteins and confocal microscopic analysis of Purα location indicate that access of Purα to the nucleus is controlled by both protein modification and sequence domains within the protein. Analyses of deletion mutants identify Purα domains mediating nuclear exclusion, including several potential destruction motifs and a PEST sequence at aa's 215–231. In the nucleus Purα colocalizes with CDK2 and cyclin A. Purα and cyclin D1, however, do not colocalize in the nucleus. At mitosis Purα is visualized about the condensed chromosomes and in the cytoplasm, where it colocalizes with cyclin B1. The data indicate that the ability of Purα to interact with proteins regulating cell proliferation and transformation is controlled by signals that govern its intracellular localization. J. Cell. Biochem. 81:621–638, 2001.

Key words: *PURA*; *ras*; colony formation; focus formation; CDK; cyclin; PEST sequence

The Pur proteins constitute a family, highly conserved among metazoan organisms, originally identified by ability of its members to specifically bind a purine-rich element in single-stranded DNA [Bergemann et al., 1992]. One family member, Purα, is now recognized as a multifunctional protein, the activities of which depend upon its ability to bind either DNA or RNA [Gallia et al., 2000]. Several publications describe the ability of Purα to act as either a transcriptional activator [Herault et al., 1992; Haas et al., 1995; Krachmarov et al., 1996; Osugi et al., 1996a; Zambrano et al., 1997] or repressor [Kelm et al., 1999; Lasham et al., 2000]. Purα stimulation of transcription of the HIV-1 genome is mediated by binding of Purα to the TAR RNA element present near the 5' end of the transcript [Chepenik et al., 1998]. Purα interacts with the promoter of the vascular smooth muscle alpha actin gene to repress transcription and can also interact with the mRNA transcript to repress translation [Kelm et al., 1999]. Purα exerts an inhibitory effect on JC viral DNA replication in human glial cells [Chang et al., 1996]. Purα co-immunoprecipitates with several proteins, including Rb [Johnson et al., 1995], cyclin A [Itoh et al., 1998] and the Tat protein of HIV-1 [Krachmarov et al.,

Grant sponsor: NIH (Instrumentation); Grant number: 1S10 RR0 9145-01; Grant sponsor: NSF (Major Research Instrumentation); Grant number: DBI-9724504; Grant sponsor: Confocal laser scanning microscopy was performed at the MSSM-CLSM core facility, supported from NIH and NSF; Grant sponsor: National Institutes of Health; Grant numbers: CA55219, NS35000.

*Correspondence to: Edward M. Johnson, Mount Sinai School of Medicine, Box 1194 Pathology, New York, NY 10029. E-mail: johnson@msvax.mssm.edu

Received 24 October 2000; Accepted 13 December 2000

This article published online in Wiley InterScience, March 19, 2001.

1996] observed to be present in the cell nucleus. The propensity of Purα to multimerize with itself [Gallia et al., 1999] and to bind Tat [Wortman et al., 2000] are both dependent upon the presence of RNA. Purα has been shown to form ternary complexes with its element in nucleic acids and certain other proteins [Johnson et al., 1995; Krachmarov et al., 1996]. Given its ability to bind a specific element in nucleic acids as well as diverse proteins, it has been speculated that one primary function of Purα may be to direct regulatory proteins to specific sites of action on nucleic acids [Itoh et al., 1998].

Considerable evidence implicates Purα in pathways controlling checkpoints in cell cycle progression. The level of Purα protein in monkey CV-1 cells varies throughout the cell cycle, rapidly declining at the onset of S phase and recovering to peak at mitosis [Itoh et al., 1998]. Purα has been shown to specifically associate with the hypophosphorylated form of Rb in G1, this complex dissociating at the G1/S transition when Rb becomes phosphorylated [Johnson et al., 1995; Itoh et al., 1998]. After dissociation of Purα and Rb, Purα levels decline. As Purα levels recover throughout late S and G2, Purα colocalizes with cyclin A in nuclear foci with newly replicated DNA, as shown by studies employing immunoelectron microscopy [Itoh et al., 1998]. Microinjection of NIH3T3 cells with purified Purα in S phase, when Purα levels are normally low, arrests cells at G2/M with fully-replicated DNA. Cells microinjected with Purα in G1 phase are either arrested without entering S phase, most of such cells undergoing a programmed cell death, or at the G2/M boundary [Stacey et al., 1999]. These data indicate that high levels of Purα can implement arrest at either G1/S or G2/M checkpoints but that they do not block ongoing DNA replication. Here we report that elevated levels of Purα markedly inhibit colony and focus formation by *ras*-transformed cells. Analysis of dynamic changes in the nuclear localization of Purα and Purα deletion mutants reveal that the ability of Purα to colocalize with cell cycle regulatory proteins is mediated by sequences in the protein that govern its nuclear localization or exclusion.

METHODS

Plasmid Constructions

An EcoRI fragment containing the complete coding sequence of Purα, derived from a λgt11 clone previously described [Bergemann et al., 1992], was cloned into the plasmid pBABEpuro, which carries the puromycin resistance gene and the Moloney murine leukemia retroviral sequence [Morgenstern and Land, 1990]. The resulting construct, pBABEpuro-purα is referred to as pBABEpurα, and the empty vector as pBABE, for clarity. In certain experiments pBABE was used in cotransfections, not to generate retrovirus, but to confer puromycin resistance. Purα and deletion mutants cloned in the pEBVHisB vector (Invitrogen Corp.), containing the Rous sarcoma virus promoter, were provided by Drs. G. Gallia and K. Khalili. They yield a fusion protein, the N-terminus of which comprises a 6-His affinity purification tag as well as an Xpress epitope tag, to add a total of 33 aa, including codons comprising the BamHI site. For direct fluorescence studies of Purα fused to green fluorescent protein, the EcoRI fragment of Purα cDNA containing the complete coding sequence, was cloned C-terminal to enhanced green fluorescent protein in the EcoRI site of the vector pEGFP-C2 (Clontech Laboratories, Inc.). The deletion mutants EGFP-C2-Purα (ΔN-85) and (ΔN-167) were produced in the same fashion. All plasmids were verified by DNA sequencing, performed by the Utah State Biotechnology Center.

Cell Culture, Cell Synchronization, and Transfections

NIH3T3 mouse fibroblasts or NIH3T3 cells transformed with K-*ras* [Kang and Krauss, 1996] were maintained in Dulbecco's modified Eagle's Medium (DMEM) supplemented with 10% (v/v) newborn calf serum, 1% (v/v) Penicillin/Streptomycin and 1% (v/v) L-Glutamine. Cells were synchronized in early S phase according to the double thymidine block method of Karn et al. [1974] modified for cell monolayers. At designated time points, cells were detached with trypsin, rinsed once in PBS and fixed in ice cold 80% ethanol. Following fixation, cells were resuspended in staining solution (0.25 mg/ml RNase A, 5 μg/ml propidium iodide in PBS). Samples were incubated in staining solution at 37°C for 30 min and analyzed using a FACScan flow cytometer and CellQuest software (Becton Dickinson). Cells were plated at 10^6 cells per 6 cm dish 12–24 h prior to transfection using 6 μg of sterile plasmid DNA and 9 μl of FuGene6 transfection reagent (Boehringer Mannheim Biochemicals). Cotransfections were

achieved with a 5-fold excess of the plasmid bearing the selectable marker over that bearing the gene of interest.

Retroviral Mediated Gene Transfer

Either pBABE or pBABEpurα were used to transfect the retroviral packaging cell line ϕNX-Eco [Kinoshita et al., 1998] as described by Pear et al. [1993]. Cells (2.5×10^6) were transfected with 6 μg of DNA using FuGene6 reagent as detailed above. After transfection, the packaging cells were cultured at 32°C to promote viral stability. Supernatant containing retrovirus, prepared as described [Pear et al., 1993], was snap frozen in liquid nitrogen and stored at −80°C. Infections of NIH3T3 cells were performed according to the method of Danos and Mulligan [1988].

Growth Curves

Pools of cells or individual clones of cells stably-transfected with either pEBV or pEBV-purα were obtained, after transfection as described above, by selection for two weeks with 500 μg/ml of hygromycin. Cells, maintained in 200 μg/ml of hygromycin, were plated in 96 well plates at a density of 100 cells per well, with at least five replicates per cell type, and grown under standard culture conditions. At 12 h intervals over a period of four days, microplates representing each time point were drained of medium and frozen at −80°C. When all samples were collected, cell number was determined using the CyQuant cell proliferation assay kit (Molecular Probes, Inc.) according to the manufacturer's protocol for adherent cells. The samples were analyzed on a Spectramax Gemini fluorescent microplate reader (Molecular Devices, Inc.).

Assay for Colony Formation Efficiency

NIH3T3 cells or *ras*-transformed NIH3T3 cells were transfected as described above, with either 5 μg of vector pBK-CMV (pBK, Stratagene) or pBK bearing a full-length Purα cDNA under control of the cytomegalovirus promoter (pBKpurα). In all cases cells were co-transfected with 1 μg of vector pBABE in order to confer puromycin resistance. Additional controls received pBABE alone. After 48 h cells were replated into 10 cm dishes and selected with 5 μg/ml puromycin for two days. Cells were then cultured in normal growth medium containing 2.5 μg/ml puromycin for an additional 11 days. Colonies were stained with crystal violet for counting.

Assay for Anchorage-Independent Cell Growth

Pools of NIH3T3 cells or *ras*-transformed NIH3T3 cells transfected with either pBABE, pBABE + pBK or pBABE + pBKpurα were obtained by selection in puromycin as described above. The selected cells were then assayed for focus formation in soft agar in 6 cm dishes. 10^4 cells were suspended in 7 ml of 0.2% Noble agar (Difco) in DMEM containing 10% newborn calf serum and this suspension was overlaid on presolidified 0.4% agar in the same medium. Normal growth medium was gently layered over the cultures every 3 to 4 days for 14 days. Colonies were stained with 2-(4-iodophenyl)-3-(4-nitrophenyl)-5-phenyltetrazolium chloride (INT) for 48 h at 37°C. Colonies were counted under a low-power inverted microscope using an ocular micrometer. For each of nine culture dishes (per experimental treatment) three fields of view were counted, at three predetermined positions, in order to minimize bias. For each data point the mean value of the three fields was calculated.

Statistical Analyses of Data

The type I error level was set at $P < 0.05$ for all tests. Planned comparisons using analysis of variance (ANOVA) were performed with Super-ANOVA software (Abacus Concepts, Inc.). Contingency tables were subjected to Chi Square (χ^2) analysis with testing for post hoc cell contributions using StatView software (SAS Institute Inc.). Where indicated, data are displayed as mean values with standard errors.

Preparation of Nuclear and Cytoplasmic Extracts

Nuclei and cytoplasm were fractionated from proliferating NIH3T3 fibroblasts according to the method of Johnson et al. [1974]. Pelleted nuclei were resuspended at 4°C in a volume of low salt buffer [25% (v/v) glycerol, 1.5 mM magnesium chloride ($MgCl_2$), 0.2 M potassium chloride (KCl), 0.2 mM EDTA, 0.2 mM phenylmethylsulfonylfluoride, 0.2 mM dithiothreitol, 1 μg/ml leupeptin, 1 μg/ml aprotinin, 20 mM Hepes, pH 7.9 at 4°C] equal to one-half the volume of the nuclear pellet. A volume of high salt buffer (identical to low salt buffer but with 1.2 M KCl) equal to that of low salt buffer was added in a dropwise fashion, with constant gentle stirring. The mixture was incubated at

4°C for 30 minutes. Extract was then subjected to centrifugation at 25,000*g* for 30 min at 4°C. The resulting supernatant was designated the nuclear extract. Cytoplasmic and nuclear fractions were assayed for protein concentration with the BCA assay system (Pierce Chemical Co.).

Immunoblot Analysis

Protein samples were resolved by SDS-PAGE and transferred to Immobilon-P (Millipore Corp.) membranes. Membranes were then treated with 5% (w/v) nonfat dry milk (Carnation) in Tris-buffered saline (TBS) for at least 2.5 h at room temperature. Blots were incubated with primary antibody in buffer A, containing 5% nonfat dry milk, 5% (v/v) horse serum (Gibco-BRL), 0.1% (v/v) Tween-20 (Sigma) for 2 h at room temperature with gentle shaking, then washed four times in TBS plus 0.1% Tween-20 (TTBS). Following a 1 h incubation with horseradish-peroxidase-conjugated secondary antibody in buffer A, the filters were again washed as above and rinsed in TBS for five minutes. Chemiluminescence was developed using the SuperSignal system (Pierce Chemical Co.). Anti-Xpress antibody was obtained from Invitrogen. Anti-histone deacetylase I was obtained from Santa Cruz Biotechnology. Monoclonal antibody against an acetylated, cytoplasmic form of α-tubulin [Piperno et al., 1987] was kindly provided by Dr. G. Piperno. Rabbit polyclonal antiserum was raised against the Purα-GST fusion protein. Whole serum was used at a dilution of 1:10,000.

Indirect Immunofluorescence or Direct Fluorescence of Cells Expressing Purα Fused to Enhanced Green Fluorescent Protein (EGFP)

NIH3T3 mouse fibroblasts, stably transfected to overexpress the epitope tag construct pEBV-purα, were seeded on glass coverslips at least 24 h before fixation, then fixed and stained according to the method of Spector and Smith [1986]. Primary antibodies were obtained from the following suppliers: anti-cyclin A (Transduction Laboratories); anti-cyclin B1, anti-cyclin D1, anti-CDK2 (Santa Cruz Biotechnology), anti-Xpress (Invitrogen). All antibodies were used at a dilution of 1 μg/ml with the exception of anti-cyclin A, which was used at 7.5 μg/ml and anti-Xpress which was diluted to 2.5 μg/ml. Fluorescein-conjugated anti-mouse IgG was diluted to a final concentration of 2.5 μg/ml, and rhodamine-conjugated anti-rabbit IgG was diluted to 5 μg/ml (Zymed Laboratories). DNA was stained with Hoechst 33342 at 0.5 μg/ml for 5 minutes. Coverslips were mounted in antifade mounting medium consisting of glycerol with 2.5% 1,4-diazabicyclo[2.2.2]octane (DABCO) and 10 mM Tris-HCl pH 7.4 and sealed with clear nail polish. Cells transfected with pEGFP constructs were fixed in 3.7% paraformaldehyde prior to visualization. Photomicroscopy and image processing were performed with a Leica TCS-SP confocal laser scanning microscope. Optical sections were imaged at 0.5 micron intervals. Channel interference from the UV laser, i.e. Hoechst signal appearing in the FITC channel, was reduced to zero with a negative density filter.

RESULTS

Expression of Purα Retards Cell Cycle Progression in Synchronous *Ras*-Transformed and Non-Transformed NIH3T3 Cells

Cells transformed by constitutively-activated *ras* reportedly undergo an accelerated G1 phase of the cell cycle due primarily to the ability of *ras* to increase levels of cyclin D1 [Albanese et al., 1995; Liu et al., 1995; Winston et al., 1996]. Since Purα acts downstream of cyclin D1 to bind Rb [Johnson et al., 1995; Itoh et al., 1998], and since microinjected Purα can block the G1-S transition [Stacey et al., 1999], we hypothesized that Purα could block this aspect of *ras* transformation. To address this question we employed cell lines stably-transfected to express Purα at levels that are in range of those normally observed in the cell cycle. We reasoned that effects of Purα thus obtained would likely be physiological effects of the protein in vivo. We employed a double-thymidine block to synchronize *ras*-transformed NIH3T3 cells and non-transformed NIH3T3 cells as well as both cell lines stably transfected to express Purα. The double thymidine block arrests the cells upon entry to S phase. The cells were released from the block into normal growth medium and samples were collected every two hours for 18 h (approximately one cell cycle). These samples were subjected to fluorescence-activated cell sorting (FACS) to determine cellular DNA content. Stably-transfected clones were selected and analyzed for Purα levels by immunoblotting (data not shown). *Ras*/3T3 pBABE + pBKpurα^{high} produces the epitope-

tagged ectopically-expressed Purα at a level approximately 5-fold greater than that of endogenous Purα. *Ras*/3T3 pBABE + pBKpurα^{low} expresses tagged Purα at a level approximately equal to that of endogenous Purα. These clonal lines, as well as pools of stably-transfected *Ras*/3T3 cells (*Ras*/3T3 pBABE + pBKpurα), were used to assess the rate of cell cycle progression in the presence or absence of excess Purα. In addition, clonal populations of NIH3T3 cells stably transfected to express the vector pEBV or the construct pEBVpurα were synchronized and analyzed in the same manner. Comparison of rows c–e of Figure 1 with row b reveals that expression of Purα retards both entry into S-phase and progression through S-phase in the *ras*-transformed cells. At 2 h post-release from the double thymidine block, *Ras*/3T3 cells transfected with pBABE vector alone (row a), as well as control cells transfected with pBABE and pBK vectors (row b), have progressed more than midway through S phase. However, cells overexpressing Purα (rows c, e) remain in very early S phase, with a significant number of cells lagging at the G1/S transition. At 4 and 6 h post-release, the effect of Purα becomes more pronounced. At 6 h the majority of cells with no pBKpurα have completed DNA synthesis to possess a 4 N DNA content. In contrast few of the cells overexpressing Purα have completed DNA synthesis, and $> 80\%$ remain in S phase (row c, rightmost panel). The effect of Purα is dose-related. The cells expressing low levels of Purα (row d) are slightly retarded in S-phase progression while the cells expressing high levels (row e) show the most pronounced retardation of any of the cells tested. *Ras*/3T3 pBABE + pBkpurα^{high} cells exhibit a marked delay in S phase progression, and a subpopulation of these cells demonstrate inhibited entry into S phase (row e, T = 6h). Vectors pBABE and pBK had no effect on cell cycle progression (row b). The pEBV vector was used for the non-transformed cells because selected pools or clones of cells overexpressing Purα from the pBK-CMV vector could not be obtained due to the cell cycle arrest induced by high levels of Purα in these cells. The level of Purα in the cells with pEBVpurα, expressed from the RSV promoter, is comparable to that in the clone pBKpurα^{low}. This level of Purα has a slight effect on the non-transformed NIH3T3 cells. Whereas at 6 h about 30% of cells with pEBV alone have completed DNA synthesis, $< 20\%$ of cells with elevated Purα expression (bottom row) have done so.

Overexpression of Purα Decreases Rate of Proliferation of NIH3T3 Cells

To demonstrate that delayed progression through S phase, mediated by Purα, results in overall decreased rate of proliferation, the growth rate of non-transformed NIH3T3 cells was analyzed. Cells were plated in 96 well plates at 100 cells per well (8 replicates per cell type) and samples were taken every 12 hours. The total number of cells per well at each time point was assayed with the CyQuant cell proliferation assay, and the results were expressed graphically (Fig. 2). Error bars represent the standard error of the mean. Over time those cells overexpressing Purα exhibit a significantly slower growth rate compared to the control cells. From 36 to 72 h cells overexpressing Purα grew at a rate only 53% that of cells with vector alone. There was little or no proliferation of cells with elevated Purα beyond 72 h. That inhibition of proliferation is an effect of Purα additional to its effects on cell cycle kinetics. Since these are stably-proliferating pools of selected cells, they are capable of proliferating in extended fashion. The cessation of growth seen here, under conditions in which cells were allowed to accumulate in the culture dish, may reflect increased sensitivity of the cells with enhanced Purα to contact inhibition or to limitation of required growth factors.

Purα Preferentially Inhibits Colony Formation by *Ras*-Transformed NIH3T3 Cells vs. Untransformed Cells

In order to assess effects of Purα on *ras* transformation that might occur in addition to effects on cell cycle kinetics, we examined colony formation by both transformed and non-transformed cells. *Ras*-transformed NIH3T3 cells or non-transformed NIH3T3 cells were cotransfected to express pBABE with either empty pBK vector or pBKpurα, as described in Methods. The cells were cultured for 14 days in selective medium, and the number of puromycin-resistant colonies were stained and counted. Six replicate dishes were plated for each sample. Figure 3A shows a single dish from each experimental group. To rule out toxic effects of Purα unrelated to cell transformation, we used non-transformed NIH3T3 cells as a control. As shown in Figure 3B, the non-transformed cells

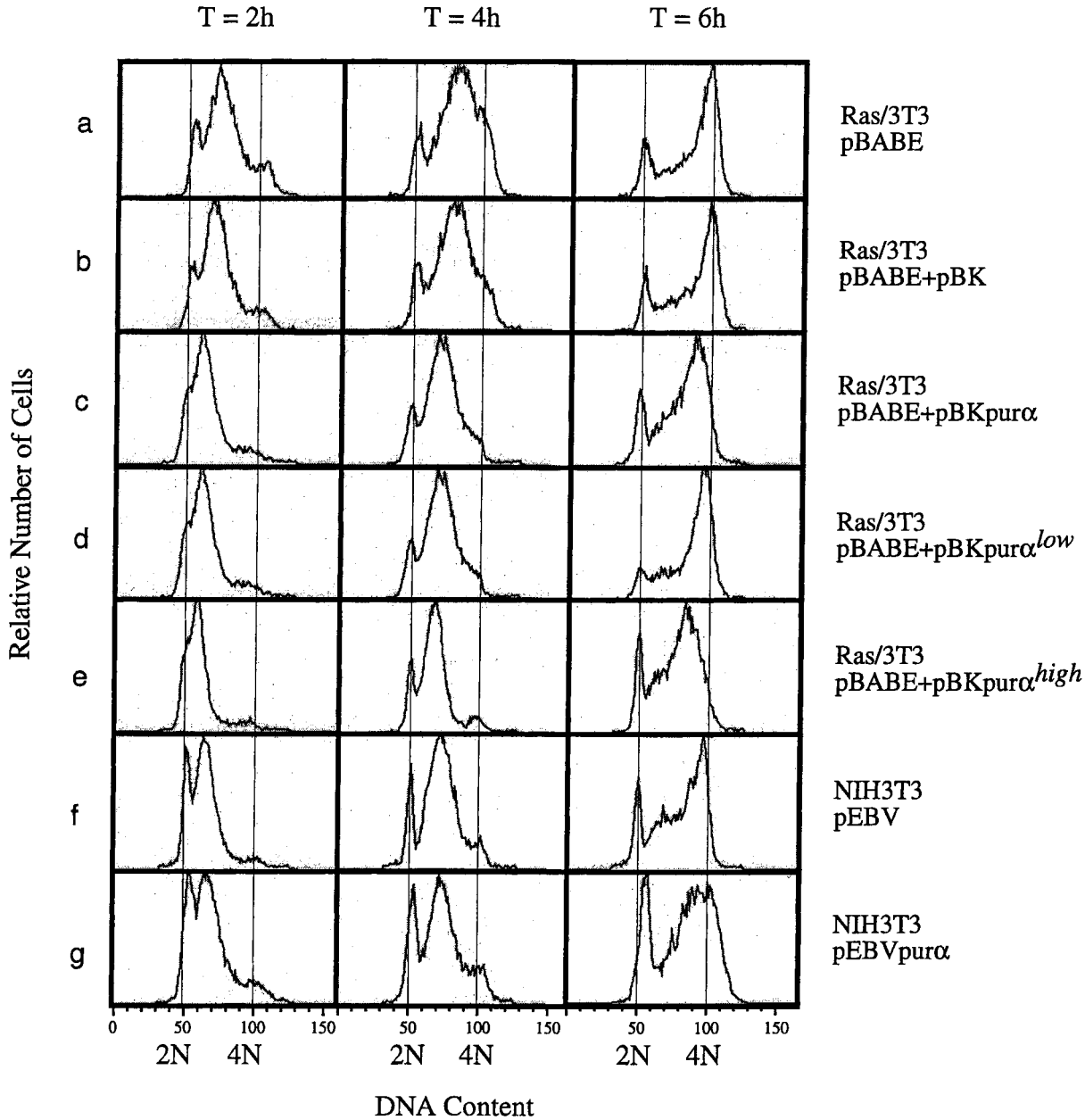

Fig. 1. Cell cycle progression in *ras*-transformed and non-transformed NIH3T3 cells transfected to overexpress Purα. Stably transfected pools and stably transfected clones are as follows: *Ras*/3T3 pBABE, pool of *ras*-transformed NIH3T3 cells stably transfected with the empty vector pBABE; *Ras*/3T3 pBABE + pBK, pool of *ras*-transformed NIH3T3 cells stably cotransfected with pBABE and empty expression vector pBK; *Ras*/3T3 pBABE + pBKpurα, pool of *ras*-transformed NIH3T3 cells stably cotransfected with pBABE and pBKpurα to overexpress Purα; *Ras*/3T3 pBABE + pBKpurα^{low}, a clonal population of *ras*-transformed NIH3T3 cells stably cotransfected with pBABE and pBKpurα expressing Purα at a level nearly that of endogenous expression; *Ras*/3T3 pBABE + pBKpurα^{high}, a clonal population of *ras*-transformed NIH3T3 cells stably cotransfected with pBABE and pBKpurα expressing Purα at a level nearly 5-fold that of endogenous Purα; NIH3T3 pEBV, a clonal population of cells stably transfected with the empty expression vector pEBV; NIH3T3 pEBVpurα, a clonal population of cells stably transfected with the vector pEBVpurα to overexpress Purα. All cell lines were synchronized to the G1/S transition using a double thymidine block as described in Methods. Cells were released into normal growth medium, and samples were collected every two hours for one complete cell cycle. Samples were fixed in 70% ethanol, treated with RNase and propidium iodide, and analyzed with a Becton Dickinson FACSCAN fluorescence activated cell sorter. Cell cycle distributions were calculated using the CellQuest software package (Becton-Dickinson). Shown here are samples obtained at two, four, and six hours (T = 2h, T = 4h, T = 6h) post release from the double thymidine block. 2N and 4N denote haploid and diploid DNA content (X axis), emphasized with fine vertical lines. Relative number of cells (Y axis) signifies the number of events as determined by FACS.

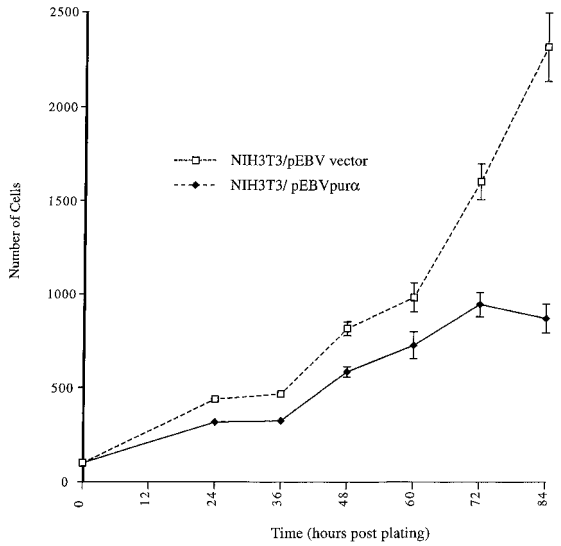

Fig. 2. Rate of proliferation of NIH3T3 cells stably transfected to overexpress Purα. Clonal populations of NIH3T3 cells stably transfected to express either pEBV vector (open squares) or pEBVpurα (closed diamonds) were plated in 96 well culture plates as described in Methods. At 12 h intervals, entire microplates representing each time point were drained of medium and stored at −80. After four days, all wells were analyzed for total cell number as described in Methods. For each time point the replicate samples were averaged, and the mean value is displayed with standard error bars. When no error bars are shown, error was so small to register.

transfected with pBABE alone formed more colonies than cells cotransfected with pBABE and the empty vector pBK (ANOVA F (1, 30) = 62.049 $P < 0.0001$). This is most likely due to the strong squelching effect of the CMV promoter present in the pBK plasmid [Reddy et al., 1995]. Non-transformed NIH3T3 cells cotransfected with pBABE and pBKpurα yielded approximately the same number of colonies as NIH3T3 cells cotransfected with pBABE and pBK (ANOVA F (1, 30) = 0.025 $P = 0.8750$). Therefore, overexpression of Purα does not inhibit colony formation in the non-transformed cells. On the other hand, *ras*-transformed NIH3T3 cells cotransfected to overexpress Purα formed 38% fewer colonies than those transfected with empty expression vector. Although when expressed in this manner the effect is not large, it is highly statistically significant (ANOVA F (1, 30) = 14.089 $P = 0.0007$). This effect of Purα is not simply a result of decreased cell proliferation. Elevated Purα levels inhibit proliferation of untransformed NIH3T3 cells (Fig. 2) whereas they have no effect on colony formation by the same cells (Fig. 3). Furthermore, the overall number of colonies of *ras*-transformed cells is reduced by Purα, not just the size of colonies. Therefore, the data indicate that cell survival of *ras*-transformed NIH3T3 cells, vs. non-transformed cells, is preferentially inhibited under conditions of colony formation by overexpression of Purα.

Overexpression of Purα Inhibits Anchorage-Independent Growth of *Ras*-Transformed NIH3T3 Cells in Soft Agar

We asked whether the selective effect of Purα on colony formation by *ras*-transfomed cells would extend to inhibition of anchorage-independent growth. Pools of *ras*-transformed NIH3T3 cells stably transfected to express Purα from pBKpurα were plated in soft agar and maintained in culture for 10 days then stained with vital dye. Stably transfected pools of non-transformed NIH3T3 cells were plated in soft agar as a control. As expected, the non-transformed NIH3T3 cells were unable to proliferate

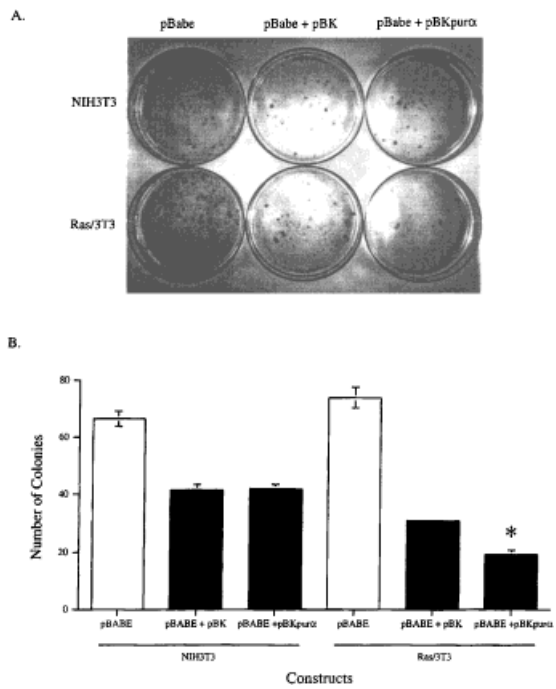

Fig. 3. Colony forming efficiency of *ras*-transformed NIH3T3 cells and non-transformed NIH3T3 cells. **(A)** Either untransformed or *ras*-transformed NIH3T3 cells were transfected with pBABE or cotransfected with pBABE and either pBK or pBKpurα. After selection with puromycin, colonies were stained and counted as described in Methods. Representative plates from one experiment are shown. **(B)** Six replicates for each sample, as described in Panel A, were averaged. The values shown represent the mean with bars to denote standard error. The asterisk indicates a statistically significant difference between the *Ras*/3T3 pBABE + pBKpurα group and the *Ras*/3T3 pBABE + pBKpurα group (ANOVA $F(1, 30) = 14.089$ $P = 0.0007$).

in the absence of adhesion, and formed no colonies in soft agar (data not shown). For each dish, three fields of view (each at the same position on the dish) were scored for the number of colonies and the average computed for each data point. This number was used to assess the total number of colonies formed, which is expressed here as a percentage of the cells initially plated (Fig. 4, top). Our findings reveal that overexpression of Purα in *ras*-transformed cells resulted in 45% fewer colonies forming in soft agar relative to cells transfected with empty vector, a statistically significant decrease (ANOVA $F(1, 24) = 45.833$ $P < 0.0001$). In addition, the individual colonies were measured using an ocular micrometer and the size distribution is expressed as three groups: less than or equal to 0.2 mm, greater than 0.2 mm but less than 1 mm, and greater than or equal to 1 mm. The size distribution of colonies formed under different transfection conditions is shown in Figure 4, bottom. Contingency table analysis of these data revealed a significant dependent relationship between the construct(s) transfected and colony size (χ^2 (df = 4, N = 300) = 30.45, $P < 0.0001$). Of the *Ras*/3T3 cells transfected with pBABE, 18% formed colonies, and 25% of those colonies were large (greater than or equal to 1 mm). Of the cells co-transfected with pBABE and pBK, 17% formed colonies, and 26% of those were large. Only 11% of *ras*-transformed cells which stably overexpressed Purα were able to form colonies, and 24% of these were less than or equal to 0.2 mm, while only 8.7% were greater than 1 mm (Fig. 4, top). Thus, the cells transfected to express Purα formed only about 1/5 the number of large colonies in soft agar as those cells transfected with control vector. This repression of anchorage independent growth correlates with the inhibition observed using the colony formation assay. These data are consistent with the notion that Purα has an inhibitory effect on the overall survival rate of *ras*-transformed NIH3T3 cells.

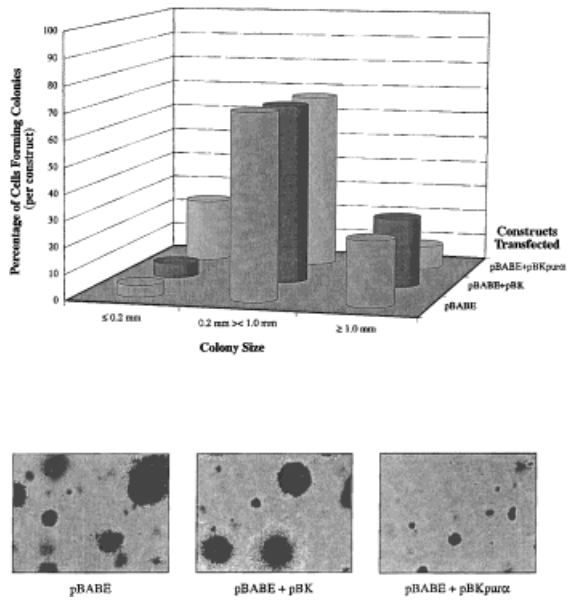

Fig. 4. Effect of Purα on anchorage-independent growth of *ras*-transformed NIH3T3 cells. *Ras*-transformed cells were transfected with either pBABE or co-transfected with pBABE and either pBK or pBKpurα and selected for puromycin resistance as described in Methods. Pools of selected cells were then plated in soft agar and cultured for two weeks. Nine replicates were plated for each sample. Colonies were stained with INT vital dye for 48 h, then colonies were counted. For each dish, the number of colonies was counted in each of three fields of view at three predetermined positions. Top: the total number of colonies formed in soft agar is expressed as a percentage of the total number of cells originally plated. The values shown represent the mean with standard error. Colonies were measured with an ocular micrometer, and the size distribution is expressed graphically in three groups: ≤ 0.2 mm (small), 0.2 mm–1.0 mm (medium), ≥ 1.0 mm (large) [X axis]. The total number of colonies formed is expressed as a percentage of the total number of cells initially plated [Z axis]. For each combination of plasmid constructs transfected [Y axis] the number of colonies in each size group is depicted. Bottom: representative photographs of colonies from each sample. Photographs are representative fields of view at equal magnification.

Purα Access to the Nucleus Involves Alterations in Purα Protein

In order to help elucidate mechanisms of Purα effects on proliferation and transformation, intracellular location and properties of the protein were examined biochemically. A retroviral infection system, vector pBABEpuro, was initially employed to study details of Purα nuclear localization since levels of Purα expressed in NIH3T3 cells from this vector would closely approximate those of endogenous Purα. The Purα expressed has no added epitope tag. NIH3T3 cells were infected with a recombinant retrovirus to express Purα or, as a control, virus expressing only the parental vector, pBABE-puro. Pools of stably infected cells were collected and lysed, and the expression of Purα was assayed by immunoblot. In uninfected NIH3T3 cells (Fig. 5A, lane 1) a rabbit polyclonal antibody to Purα recognizes a single band, representing the presence of endogenous Purα in

NIH3T3 cells. When infected to overexpress Purα (Fig. 5A, lane 2), NIH3T3 cells reveal a band of the same molecular weight, although of greater intensity, signifying that Purα, overexpressed without additional sequences fused to the primary amino acid sequence, migrates at the same size as endogenous Purα protein but is expressed to a greater degree. The predicted size of Purα based on amino acid sequence is 35 kDa, which is in contrast with the observed molecular weight of about 45 kDa. The possibility that this discrepancy is due, at least in part, to posttranslational modification is supported by the demonstration that Sf9 cells infected with a baculovirus construct to overexpress Purα produce two polypeptides, observed on immunoblot as a doublet migrating at 40–46 kDa [Itoh et al., 1998].

Further experiments were performed with Purα expressed from a CMV promoter, which produces Purα at a much higher level than does the retroviral vector. In NIH3T3 cells transiently (data not shown) or stably cotransfected (Fig. 5B) with pBABE and pBKpurα to overexpress Purα fused to the amino terminal HA tag, Purα is visualized by immunoblot as a doublet at approximately 46 kDa, with the majority of the protein existing as the faster-migrating species (Fig. 5B, lane 3). In lysates of NIH3T3 cells stably transfected with the control vectors pBABE or pBABE and pBK, (Fig. 5B, lanes 1 and 2, respectively) endogenous Purα is visualized as a single band migrating at 46 kDa. The same result is obtained with CV1, HeLa, and Cos7 cells. These observations indicate that vast overexpression of Purα cDNA generates a form of the protein that migrates faster than the bulk of the endogenous form, and that the production of a faster-migrating band is not cell type or species specific. The difference in migration between the overexpressed and endogenous Purα may reflect the higher level of the overexpressed protein, which could exceed levels of an associated protein or cofactor required to modify Purα.

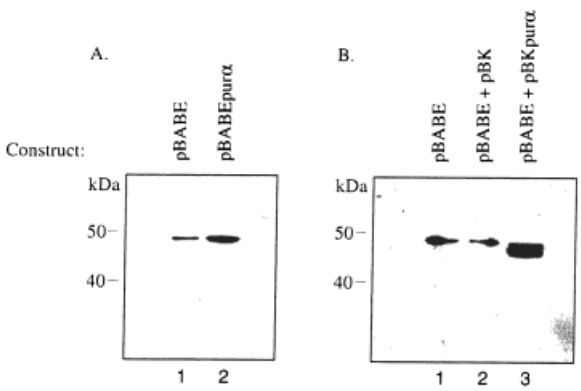

Fig. 5. Electrophoretic comparison of endogenous NIH3T3 Purα with Purα overexpressed from plasmid or retroviral vectors. **(A)** NIH3T3 cells were infected with a retrovirus to express either empty vector (lane 1, pBABE) or to overexpress Purα (lane 2, pBABEpurα). Cell extracts were prepared as described in Methods and subjected to SDS gel electrophoresis on an 8% polyacrylamide gel with molecular weight standards (Gibco-BRL). Immunoblots of cell lysate were probed with anti-purα polyclonal antisera followed by horseradish peroxidase-coupled rat anti-rabbit antibody (Zymed). **(B)** NIH3T3 cells transiently transfected to express either empty vector (lane 1, pBABE), cotransfected to express empty vectors pBABE and pBK (lane 2) or cotransfected to overexpress Purα (Lane 3, pBABE + pBKpurα). Samples were electrophoretically separated and immunoblots prepared as described in Methods.

Endogenous Purα was originally isolated from HeLa cell nuclei [Bergemann and Johnson, 1992], and has been purified from the nuclei of AKR-2B mouse fibroblasts [Kelm et al., 1997] as well as from mouse cerebellar nuclei [Osugi et al., 1996b]. Previous immunofluorescence microscopy studies have localized Purα to both the nuclei and cytoplasm of neuronal cell lines, and predominantly to the nuclei of C6 glioma cells [Osugi et al., 1996b]. In CV-1 cells, endogenous Purα was localized to nuclear foci using immunoelectron microscopy [Itoh et al., 1998]. To determine whether overexpressed Purα is primarily nuclear or cytoplasmic, nontransfected NIH3T3 cells and pEBVpurα/3T3 cells were fractionated into nuclear and cytoplasmic extracts. Equal amounts of protein, as determined by the BCA assay, were loaded on a 12% SDS-polyacrylamide gel and the presence of Purα was detected with either polyclonal antiserum against Purα or the anti-Xpress monoclonal antibody against the epitope tag. Control lysates were blotted with anti-histone deacetylase I to detect leakage of nuclear proteins into the cytoplasmic extract, or with a monoclonal antibody against a post-translationally modified form of α-tubulin present only in the cytoplasm to test for contamination of the nuclear extract with cytoplasmic protein. Both controls confirmed the integrity of the extracts (Fig. 6, lower two panels). In NIH3T3 cells Purα is a nuclear protein migrating at 46 kDa (Fig. 6, lane 2). In pEBVpurα/3T3 cells, stably transfected to overexpress Purα fused to the amino terminal Xpress tag, Purα-Xpress exists in both the nucleus and the cytoplasm, while endogen-

ous Purα is present only in the nuclear fraction. The epitope-tagged Purα is recognized by both the anti-Purα polyclonal and the anti-Xpress monoclonal antibodies. Purα-Xpress is resolved as a doublet at approximately 46 kDa, migrating with greater mobility than the endogenous Purα (Fig. 6, lanes 4 and 6). Significantly, the smallest species of Purα-Xpress, migrating at approximately 45 kDa is almost entirely cytoplasmic. This finding suggests that it is primarily a modified, slower-migrating form of Purα which localizes to the nucleus. It is conceivable that modification of Purα is necessary for either nuclear transport or nuclear retention. Overexpression of Purα-Xpress may result in a fraction of unmodified protein which is detected in the cytoplasm. Systematic analysis of all potential modifications of Purα is beyond the scope of this paper, and at this point other explanations for a slower-migrating form of Purα cannot be ruled out. Modifications are further considered in the discussion.

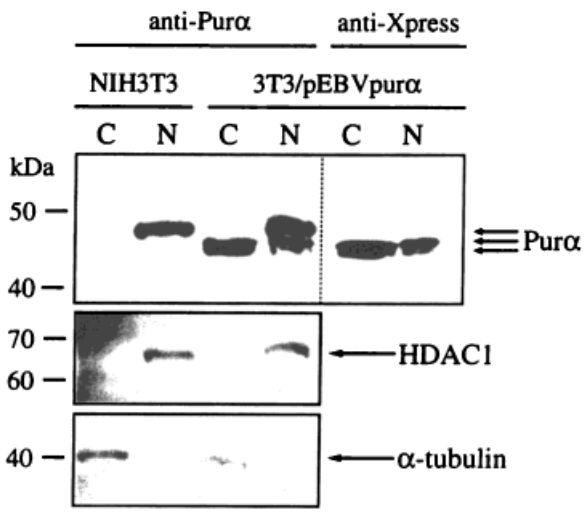

Fig. 6. Comparison of the nuclear and cytoplasmic distribution of endogenous Purα with that of Purα expressed from pEBVpurα. Nuclear and cytoplasmic fractions were prepared from NIH3T3 cells or NIH3T3 cells stably transfected to overexpress Purα-Xpress (pEBVpurα/3T3) as described in Methods. Cytoplasmic (C) and nuclear (N) fractions were separated on a 12% polyacrylamide gel, transferred to PVDF membrane and blotted with anti-Purα polyclonal antiserum or with anti-Xpress monoclonal antibody, which recognizes only the overexpressed, epitope-tagged form of Purα. To control for adequate separation of nuclei and cytoplasm, identical, parallel immunoblots were probed with either antibody against histone-deacetlyase 1(HDAC1), found only in the nucleus, or antibody against a post-translationally modified form of α-tubulin found only in the cytoplasm.

Sequences in Purα Mediate Nuclear Exclusion

Two series' of Purα deletion mutants were employed to analyze sequences involved in Purα nuclear retention or exclusion. One series was constructed with Purα or its mutants fused C-terminal to a 3 kDa Xpress epitope tag. The second series was constructed with Purα or its mutants fused C-terminal to the much-larger, 27 kDa enhanced green fluorescent protein (EGFP). Cells were analyzed with a laser scanning confocal microscope (Fig. 7). For the first series immunolocalization was performed on pEBVpurα/NIH3T3 cells. Cells transfected with empty vector expressed only the 3 kDa Xpress peptide, which diffused throughout the cell (Fig. 7A). It can be seen that full-length Purα-Xpress localized to both the nucleus and cytoplasm of proliferating cells (Fig. 7B,C), being primarily cytoplasmic in the most fluorescent cells (Fig. 7B). These cells were not synchronized, but by far the majority would be in mid to late G1, a time when Purα levels begin to decline in the nucleus [Itoh et al., 1998]. The deletion mutant pEBVpurα(ΔN-167) also localized largely to the cytoplasm (Fig. 7D). The mutants pEBVpurα(Δ72-231) (Fig. 7E) and pEBVpurα(ΔC-108) (Fig. 7F) localized almost entirely to the nucleus with strong nucleolar staining. Non-transfected NIH3T3 cells did not react with the anti-Xpress antibody (Fig. 7G). Cells treated only with the FITC-conjugated secondary antibody also showed no fluorescence, indicating an absence of non-specific interactions (Fig. 7H).

For the series of mutants fused to EGFP, expression of EGFP alone was used as a control, and mock-transfected NIH3T3 cells were used to assess autofluorescence. The results shown in Figure 7I–L are from transient transfection of NIH3T3 cells. EGFP alone, expressed by the pEGFP-C2 vector, is able to diffuse throughout the cell (Fig. 7I). EGFP-Purα is visualized only in the cytoplasm, with minimal signal in the nucleus above that of autofluorescence (Fig. 7J). EGFP-Purα(ΔN-85) is seen in both the nucleus (but not the nucleolus) and the cytoplasm, with the majority of the protein localized in the cytoplasm (Fig. 7K). EGFP-Purα(ΔN-167) is present in the nucleus and the cytoplasm in nearly equal proportion (Fig. 7L).

The data derived from deletion mutants allow two conclusions: 1) protein size is not an overriding factor in Purα access to the nucleus; and

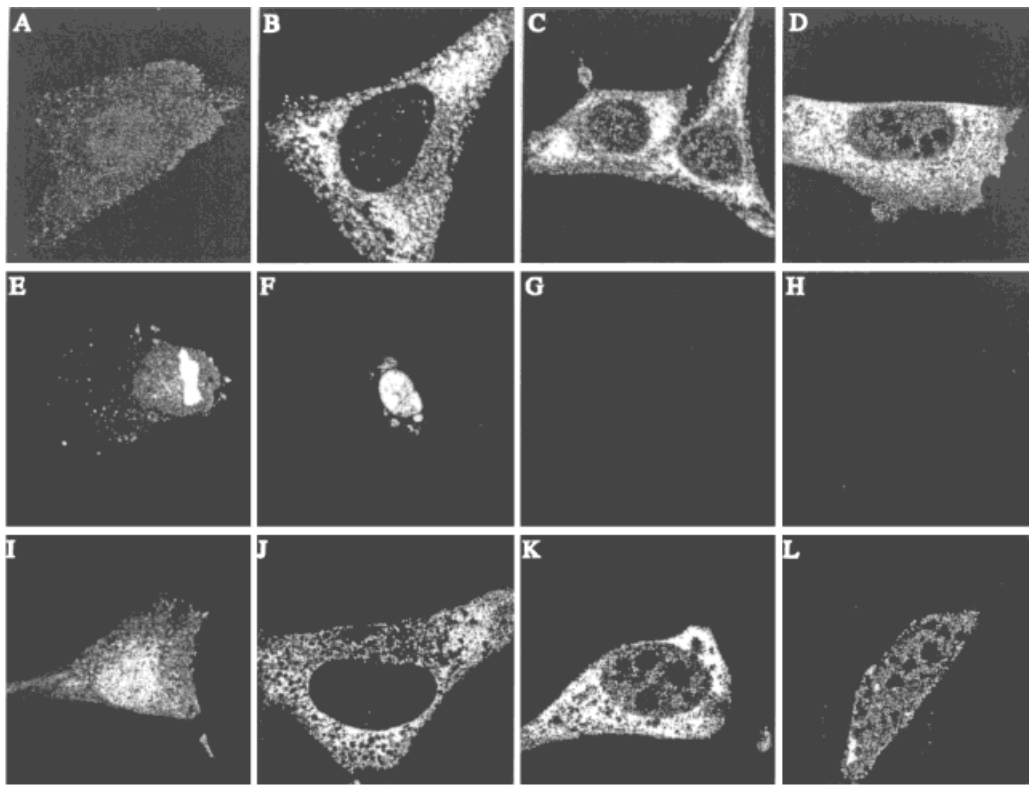

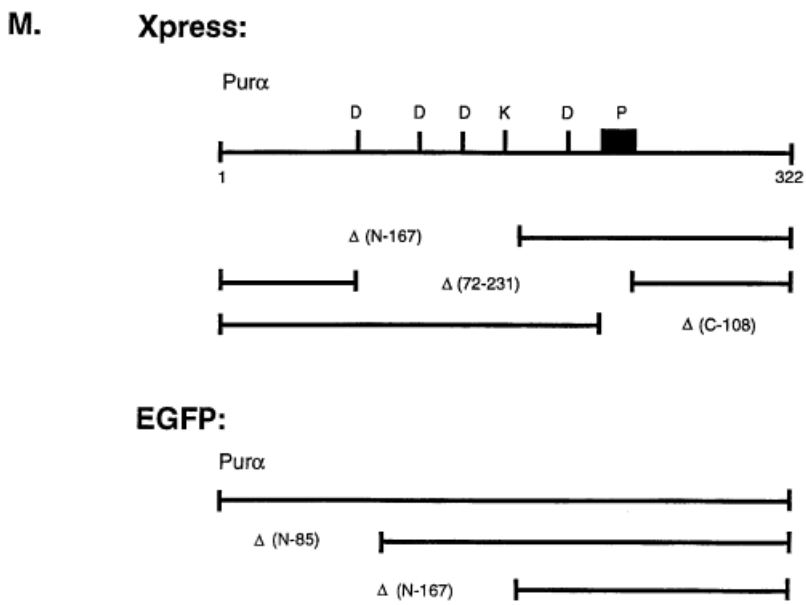

Fig. 7. Deletion analysis of the effects of molecular domains of Purα on subcellular localization. Deletion mutants of the Purα cDNA were generated as clones in either vector pEBV or vector pEGFP-C2 as described in Methods. Using these vectors Purα is expressed either with an N-terminal Xpress epitope or with a fused N-terminal enhanced green fluorescent protein, respectively. After transfection, fluorescence was visualized either indirectly, using anti-Xpress antibody and fluorescent secondary antibody, or directly, by excitation of the green fluorescent protein. Each image represents a single optical section of transiently-transfected NIH3T3 cells obtained by confocal laser scanning microscopy. The cells shown were transfected and treated as follows: **(A)** vector pEBV, treated with anti-Xpress monoclonal antibody followed by FITC-conjugated goat anti-mouse (*aX*); **(B)** pEBVpurα, *aX*; **(C)** pEBVpurα, *aX*; **(D)** pEBVpurα(ΔN-167), *aX*; **(E)** pEBVpurα(Δ72-231), *aX*; **(F)** pEBVpurα(ΔC-108), *aX*; **(G)** non-transfected NIH3T3 cells, *aX*; **(H)** stably transfected pEBVpurα/3T3 cells treated only with the FITC-conjugated goat anti-mouse secondary antibody; **(I)** pEGFP-C2 to express the 27 kDa GFP protein; **(J)** pEGFP-C2-Purα; **(K)** pEGFP-C2-Purα(ΔN-85); **(L)** pEGFP-C2-Purα(ΔN-167). Panel **M** depicts full-length Purα and its deletion mutants, fused C-terminal to either the Xpress eiptope tag (3 kDa) or EGFP (27 kDa). Positions are indicated of: potential cyclin-like destruction boxes [King et al., 1996], all possessing the motif RxxL (D); a potential KEN box [Pfleger and Kirschner, 2000] possessing the sequence KEN (K); a potential PEST sequence [Rechsteiner and Rogers, 1996] of 15 aa possessing P,E,S, and T residues (P).

2) specific sequences in Purα mediate its nuclear exclusion. The fusion of Purα with GFP produces a protein with a predicted size of approximately 65 kDa, while the deletion mutants GFP-Purα(ΔN-85) and GFP-Purα(ΔN-167) have predicted molecular weights of approximately 57 kDa and 47 kDa, respectively. This last protein is approaching the maximum size believed to allow diffusion through nuclear pores. A comparison of the two Purα(ΔN-167) mutants fused either to Xpress, Figure 7, panel D, or to EGFP, Figure 7, panel L reveals that adding more than 20 kDa to the protein, as in panel L, does not hinder its ability to enter the nucleus. While a small size is thus not an overriding factor in Purα ability to enter the nucleus, it is clear from both series' of mutants that removal of sequences from 1 to 167 progressively allows better Purα nuclear access. A comparison of Xpress fusion proteins Purα (ΔN-167), (Δ72-231) and (ΔC-108) is revealing. The first of these remains primarily cytoplasmic, while the latter two are exclusively nuclear. This indicates the particular importance of a sequence between aa's 214 and 231 in mediating Purα exclusion from the nucleus. This sequence is PAELPEGTSLTVDNKRF, a potential PEST sequence. Such sequences have been implicated in targeting proteins for degradation via a proteosome-mediated pathway [Rechsteiner and Rogers, 1996].

Purα Colocalization With Specific Cyclin/CDK Complexes is Dynamically Altered in the Cell Cycle

In addition to the above biochemical fractionation, Purα intracellular localization was analyzed by confocal laser microscopy. Immunogold electron microscopy had previously demonstrated a close association of Purα with cyclin A and newly-replicated DNA in subnuclear chromatin structures in CV-1 cells [Itoh et al., 1998]. Here, localization of Purα, and its colocalization with additional cyclins and CDKs that control different points in cell cycle progression, were examined. To study cell cycle-specific localization, pEBVpurα/3T3 cells plated on coverslips were synchronized with a double-thymidine block, and fixed at regular time points. The cells were treated with antibodies directed against the Xpress epitope attached to Purα and with antibodies directed against CDK2, cyclin A, cyclin B1 or cyclin D1. For this study, presented in Figure 8, fluorescence of the secondary antibody for Purα appears green, and that for each cyclin or CDK appears red. Confocal laser scanning microscopy enabled the visualization of single optical sections so that regions of protein colocalization could be precisely defined. Merging the green and red optical channels reveals areas of colocalization, which appear yellow. Each row across in Figure 8 presents the same field of view with different optical channels. Staining of chromatin with Hoechst 33342 (Fig. 8, A,Q) is shown for rows A–D and Q–T. To control for autofluorescence and non-specific antibody binding, the pEBVpurα/3T3 cells were stained with primary antibody alone (Fig. 8E) or secondary antibody alone (Fig. 8I), and non-transfected NIH3T3 cells were stained with the antibody against the Xpress epitope (Fig. 8M). Previous reports have indicated that CDK2 and cyclin A are primarily localized to the nucleus [Pines and Hunter, 1991] and that during S phase they localize to sites of chromosomal DNA replication [Cardoso et al., 1993]. Endogenous CDK2 is visualized primarily in the nucleus, but excluded from the nucleoli in asynchronous cells (Fig. 8C) and in cells synchronized to the G1/S transition (not shown). Purα-Xpress is visualized primarily in the cytoplasm of the same cell but also distinctly in the nucleus (Fig. 8B). Since this is a single confocal optical section, the nuclear staining is not due to cytoplasmic overlayering of the nucleus. The bulk of Purα staining in the nucleus colocalizes with that of CDK2, as shown by the presence of yellow color in Fig. 8D. It has been previously reported that nuclear levels of Purα are very low in early S phase and that Purα and cyclin A colocalize to replication foci in late S phase. In the present study, in S-phase cells the majority of overexpressed Purα is distributed in the cytoplasm while a fraction of the cellular Purα-Xpress is present in discrete nuclear foci (Fig. 8F). Cyclin A is predominantly nuclear, but non-nucleolar (Fig. 8G). Purα colocalizes with cyclin A in these nuclear foci and throughout the nucleus (Fig. 8H). The colocalizations of Purα with CDK2 (Fig. 8D) and cyclin A (Fig. 8H) are quite consistent. In both cases bright non-nucleolar foci are seen. Also in both cases there is considerable red staining in addition to yellow in the nucleus, indicating that not all CDK2 or cyclin A are associated with Purα.

Colocalization of Purα with cyclin D1 was examined since cyclin D1/CDK4 are implicated

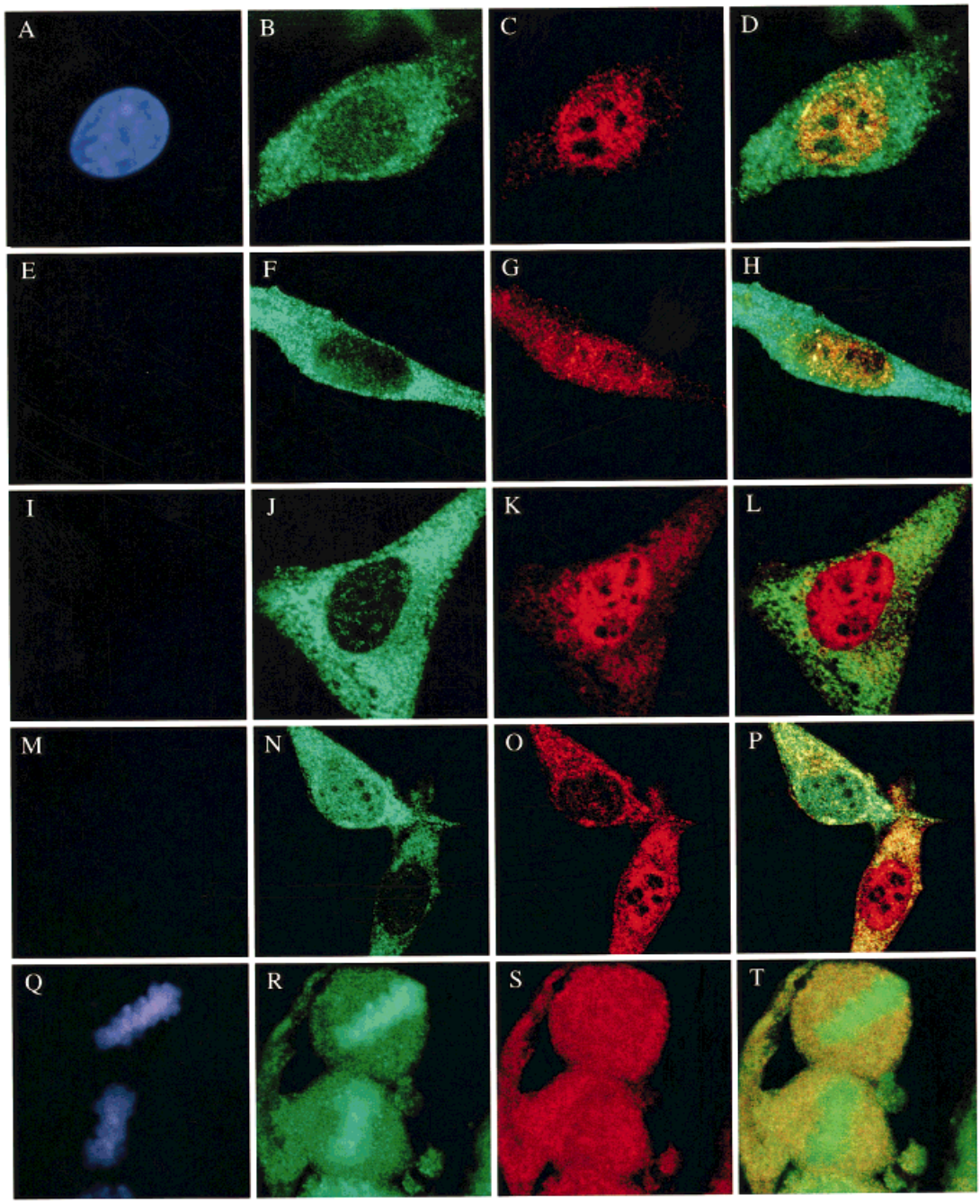

Fig. 8. Intracellular colocalization of Purα with cyclins or CDKs involved in different cell cycle transitions. Immunofluorescence confocal laser microscopy was used to assay for the colocalization of Xpress-Purα and specific cell cycle regulatory proteins in NIH3T3 cells stably transfected to overexpress Purα (pEBVpurα/3T3). Fixation, staining, and confocal microscopy were performed as detailed in Methods and in the legend to Figure 7. A–D show the same cell from an asynchronous population visualized to detect different stains. **(A)** Nucleus stained with Hoechst 33342. **(B)** Anti-Xpress + FITC-conjugated anti mouse to detect Xpress-Purα (*aX*). **(C)** Anti-CDK2 + Rhodamine-conjugated anti-rabbit to detect endogenous CDK2. **(D)** Merged FITC and Rhodamine signals. Yellow denotes colocalization of Purα and CDK2 **(E)** Non-transfected NIH3T3 cells treated with αX. F–G show the same cell from a population of cells synchronized in S phase, visualized to detect different stains. **(F)** *aX*. **(G)** Anti-cyclin A + Rhodamine-conjugated anti-rabbit to detect endogenous cyclin A. **(H)** Merged FITC and Rhodamine signals. Yellow denotes colocalization of Purα and cyclin A **(I)** pEBVpurα/3T3 cells treated with Rhodamine-conjugated anti-rabbit and FITC-conjugated anti-mouse to detect non-specificity of the secondary antibodies. Rows **J–L** and **N–P** each show the same synchronous cells at the G1/S transition visualized to detect different stains. (J, N) *aX*. J is a color view of the cell shown in Figure 7B. (K, 0) Anti-cyclin D1 + Rhodamine-conjugated anti-rabbit to detect endogenous cyclin D1. **(P)** Merged FITC and Rhodamine signals. Yellow denotes colocalization of Purα and cyclin D1. Q-T show the same synchronous cells in mitosis. **(Q)** Treated with Hoechst 33342 to stain chromatin. (R) *aX*. **(S)** Anti-cyclin B1 + hodamine-conjugated anti-rabbit to detect endogenous cyclin B1. **(T)** Merged FITC and Rhodamine signals. Yellow denotes colocalization of Purα and cyclin B1.

in phosphorylation of Rb [Ewen et al., 1993; Kato et al., 1993], which itself culminates in release of Purα. Cyclin D1 accumulates in the nucleus throughout G1, and rapidly exits into the cytoplasm in early S phase [Diehl et al., 1998]. Prominently or exclusively cytoplasmic cyclin D1 has been reported in certain tumor cells [Palmqvist et al., 1998; Dhar et al., 1999]. Cells in rows J–L and N–P were all examined at the G1/S transition. At this time the presence of Purα or cyclin D1 in the nucleus is essentially mutually exclusive. In a cell in which cyclin D1 is nuclear (Fig. 8K, 8O bottom), Purα-Xpress is largely excluded from the nucleus (Fig. 8J, 8N bottom). In a cell in which cyclin D1 is largely cytoplasmic (Fig. 8O top), Purα-Xpress is distributed throughout the cell, with the majority of the protein present in the nucleus (Fig. 8N top). Purα-Xpress colocalizes noticeably with cyclin D1 in the cytoplasm, but is virtually exclusive of cyclin D1 in the nucleus (Fig. 8L, 8P). The juxtaposition of two cells with such mutually exclusive nuclear localization of Purα and cyclin D1 as those in Figure 8, row N–P, affirms that G1/S is a point at which both proteins are changing rapidly. We have previously reported that the level of endogenous Purα declines precipitously in late G1/early S phase when Purα is dissociated from the nuclear protein Rb [Itoh et al., 1998]. One possible explanation for the data in Figure 8L and P is as follows: in late G1 when cyclin D1 is nuclear, Purα has already been dissociated from Rb, upon phosphorylation in mid G1, and due to degradation and/or nuclear export, is at very low levels in the nucleus (Fig. 8, panels J and N, bottom). In S phase, however, when cyclin D1 is exported to the cytoplasm, Purα-Xpress is distributed throughout the cell, with a significant proportion of the protein present in the nucleus (Fig. 8, panel N, top).

Colocalization of Purα with cyclin B1 was examined because the levels of the two proteins both peak at mitosis. The localization of cyclin B1 varies with the cell cycle. Cyclin B1 accumulates almost exclusively in the cytoplasm, where it is retained until the onset of mitosis [Pines and Hunter, 1991; Hagting et al., 1998; Yang et al., 1998]. In late prometaphase, the cyclin B1/CDK1 complex rapidly enters the nucleus. In a population of NIH3T3 fibroblasts synchronized to enrich for mitotic cells, those cells exhibiting nuclear cyclin B1 and condensed chromatin were considered to be in prometaphase. In these prometaphase cells, when cyclin B1 is localized to the nucleus (Fig. 8S), Purα-Xpress staining correlates with Hoechst 33342 stained-chromatin (Fig. 8R and Q, respectively), indicating that Purα is present on or very near the condensed chromosomes. Purα-Xpress colocalizes with cyclin B1 throughout the cell and at the periphery of the chromosomes, revealed here by yellow color (Fig. 8T). The peak in levels of Purα at mitosis and its location with condensed chromosomes suggest a potential role for this protein at mitosis.

DISCUSSION

The present results indicate that Purα antagonizes colony formation and anchorage-independent growth related to K-*ras* transformation of NIH3T3 cells. Cellular *ras* protein plays an important role in transducing mitotic signals to the cell cycle machinery, acting specifically at the G1 to S phase transition [Mulcahy et al., 1985]. Cells transformed by a mutant, constitutively activated *ras* gene exhibit accelerated progression through G1 phase [Filmus et al., 1994; Albanese et al., 1995; Liu et al., 1995; Arber et al., 1996; Winston et al., 1996; Aktas et al., 1997; Kawada et al., 1997]. Ectopic expression of cyclin D1 has been shown to result in a shortened G1 phase [Quelle et al., 1993; Resnitzky, 1997] and anchorage independent growth in rodent fibroblasts [Resnitzky, 1997]. Activated *ras* also up-regulates cyclins A, D3 and E1 [Fan and Bertino, 1997], and *ras*-dependent cyclin A induction is important for anchorage independent growth [Kang and Krauss, 1996]. Since Rb hyperphosphorylation is induced at least in part by cyclin D1/CDK4 (see Sherr and Roberts, 1995; Weinberg, 1995 for reviews), *ras* signaling pathways may in part control the association of Rb and Purα.

One major difference between Purα and other Rb-binding proteins is that upon release from Rb in late G1, Purα levels decline [Itoh et al., 1998]. Therefore, artificially raising intracellular levels of Purα can provide clues to the cellular function of this decline. The results of Figure 1, achieved by stable transfection to express Purα, are consistent with results obtained by microinjection of Purα [Stacey et al., 1999] and further illuminate potential mechanisms of cell cycle hindrance. In the previous studies, microinjection of Purα in G1 phase arrested a high proportion of cells at the G1-S

boundary leading to a programmed cell death. In the present study, the lower levels of Purα in the stably-transfected lines did not fully arrest the cycle, but significantly retarded the progression of the cycle at the same point. Taken together, the results indicate a progressive, dose-dependent action of Purα to inhibit the onset of S-phase. Upon microinjection in S or G2, Purα induced a G2-M arrest but did not prevent complete replication of the genome. In the present study the lower levels of Purα do not cause a complete arrest of the cycle, but they do retard progression of the cells through S-phase. Again, however, Purα does not prevent cells from completing replication of the genome. Taken together, the results indicate an inhibitory action of Purα that does not compromise the DNA synthetic machinery. Results thus indicate that a decline in Purα levels may be necessary for progression of cells into S-phase.

While the present results document effects of elevated Purα at cell cycle transition points, they do not identify the exact role of the protein in inhibiting either G1/S or G2/M transitions. Analyses of the intracellular localization of Purα at different times in the cell cycle and of its associations with cell cycle regulatory proteins provide clues regarding potential molecular functions of the protein.

Localization studies suggest that Purα may affect the cell cycle as cells approach mitosis. Purα has been shown to coimmunoprecipitate and colocalize with cyclin A and newly-replicated DNA during late S and G2 phases of the CV-1 cell cycle [Itoh et al., 1998]. Here we report that exogenously-expressed Purα also colocalizes with cyclin A, and with CDK2, in the nucleus. The bulk of the exogenously-expressed Purα, however, is present in the cytoplasm (Fig. 8B,F,J). It is clear from the juxtaposition of cells (see Fig. 8, N–P) that cell cycle timing involves rapid changes in localization of the exogenously-expressed Purα to the nucleus, particularly at the G1/S transition. At mitosis Purα levels are high throughout the cell and particularly on or about the condensed chromosomes. Purα colocalizes with cyclin B1 in the cytoplasm and at the periphery of the chromosomes. These data suggest a role for Purα in the progression of newly-replicated DNA through mitosis. Such a role could include function of the single-stranded DNA-binding activity of Purα in monitoring and in repair or recombination of ineffectively-replicated DNA or in preventing re-replication of once-replicated DNA. Hindrance of S-phase progression by elevated levels of Purα could, thus, stem from its interference with the replication apparatus or from lack of displacement of the protein from specific sites on the DNA. This would explain the necessity of Purα disappearance at the onset of DNA replication. This inhibitory effect is also consistent with previous observations that Purα inhibits JC virus DNA replication in glial cells [Chang et al., 1996]. Studies currently underway to assess the disposition of mice with genetically inactivated *PURA* will shed further light on the functions of the encoded protein.

It should be noted that endogenous cytoplasmic Purα has been seen in cells [Osugi et al., 1996b; Tretiakova et al., 1999]. Furthermore, Purα associates with RNA as well as DNA [Herault et al., 1995; Gallia et al., 1999; Kelm et al., 1999; Wortman et al., 2000]. Purα has been reported to associate with RNA transcripts of certain genes believed to be regulated by promoter *PUR* elements [Chepenik et al., 1998; Kelm et al., 1999]. It is conceivable that effects of Purα on *ras* transformation could be mediated, in addition to its demonstrated effects in the nucleus, by interaction with RNA in the cytoplasm.

Fluctuations in Purα levels and ensuing cell cycle regulatory effects may become aberrant in instances of disruption of the gene encoding Purα, *PURA*. The human *PURA* gene is located at chromosome band 5q31 [Ma et al., 1995], a site frequently deleted in acute myelogenous leukemia (AML) [Pederson and Jensen, 1991; Le Beau et al., 1993]. Recently we have observed *PURA* deletions in $> 95\%$ of patients with myelodysplastic syndrome (MDS) that have 5q abnormalities [Lezon-Geyda et al., 1997]. Mutations in Rb are rare in AML, but it is conceivable that Purα functions in a pathway mediating an aspect of Rb control and that alterations in Purα levels could influence checkpoint control.

The present results indicate that access of Purα to the nucleus is under complex control potentially involving both post-synthetic modification and nuclear exclusion. Figures 5 and 6 indicate that the endogenous, nuclear form of Purα migrates slower on an SDS gel than does a largely cytoplasmic form observed upon vast overexpression. A systematic analysis of all Purα modifications has not been done, but there is evidence, not shown here, that the protein is modified. A slower-migrating form of Purα has

been shown to react with anti-phosphoserine antibody, and when excised from a gel, to contain phosphoserine and phosphothreonine by amino acid analysis. Purα contains 32 S and T residues, many of them in consensus sequences for various protein kinases. Interestingly, Purα contains no CDK consensus sequences, and Purα is not phosphorylated by purified cyclin A and CDK2, a protein with which PurA is seen to colocalize (Fig. 8). Modifications of Purα in addition to phosphorylation are also possible. Purα does not possess a canonical nuclear localization signal, and results in Figure 7 do not provide clear evidence for one. Purα may enter the nucleus by diffusion, since it is small enough to traverse nuclear pores, or by co-transport with known nuclear protein partners. Results in Figure 7 indicate that below about 47 kDa, protein size is not an overriding factor in Purα nuclear localization. Therefore, nuclear retention is likely to be mediated by sequence domains within the protein. Purα possesses four RxxL sequences, certain of which are very homologous to cyclin A and B1 destruction boxes [King et al., 1996], a KEN box [Pfleger and Kirschner, 2000] and a PEST sequence [Rechsteiner and Rogers, 1996]. As indicated in Figure 7M, these are all located in a region of Purα which, when deleted progressively, confers greater nuclear retention upon the protein. The PEST sequence, in particular, may be important since it alone evidently assigns nuclear exclusion to mutant Purα (ΔN-167). Each of these categories of sequence motifs can target a protein for ubiquitin-mediated degradation. The mutational analysis carried out here thus suggests the possibility that Purα may be excluded from the nucleus at specific times in the cell cycle via targeting of the nuclear protein for proteolysis. The Purα PEST sequence of 15 aa contains 3 S and T residues, which are potential phosphorylation sites. It is conceivable that modifications of Purα, including the PEST sequence, KEN or destruction boxes, could distinguish cytoplasmic from nuclear forms of the protein and facilitate targeting of the latter for proteolytic descruction. Casein kinase 2-catalyzed phosphorylation of a PEST sequence has been implicated in directing nuclear vs. cytoplasmic distribution of nucleosome assembly protein 1 in HeLa cells [Li et al., 1999]. KEN-box-dependent proteolysis of CDC6 has been implicated in licensing of replication origins in the nucleus [Petersen et al., 2000]. The present results underscore the necessity for a thorough analysis of Purα modification sites and of the mechanism by which Purα levels decline in the nucleus during the cell cycle.

ACKNOWLEDGMENTS

Fluorescence-activated cell sorting was expertly performed by Dr. John Hirst at the flow cytometry facility of the Kaplan Cancer Center of the New York University School of Medicine. We thank Dr. Robert Krauss for providing K-*ras*-transformed NIH3T3 cells, and Dr. Gianni Piperno for the gift of anti-α-tubulin antibody. The pEBV constructs were generated Dr. Gary Gallia, and generously provided by Dr. Kamel Khalili.

REFERENCES

Aktas H, Cai H, Cooper GM. 1997. Ras links growth factor signaling to the cell cycle machinery via regulation of cyclin D1 and the Cdk inhibitor p27KIP1. Mol Cell Biol 17:3850–3857.

Albanese C, Johnson J, Watanabe G, Eklund N, Vu D, Arnold A, Pestell RG. 1995. Transforming p21ras mutants and c-Ets-2 activate the cyclin D1 promoter through distinguishable regions. J Biol Chem 270: 23589–23597.

Arber N, Sutter T, Miyake M, Kahn SM, Venkatraj VS, Sobrino A, Warburton D, Holt PR, Weinstein IB. 1996. Increased expression of cyclin D1 and the Rb tumor suppressor gene in c-K-ras transformed rat enterocytes. Oncogene 12:1903–1908.

Bergemann AD, Johnson EM. 1992. The HeLa Pur factor binds single-stranded DNA at a specific element conserved in gene flanking regions and origins of DNA replication. Mol Cell Biol 12:1257–1265.

Bergemann AD, Ma ZW, Johnson EM. 1992. Sequence of cDNA comprising the human pur gene and sequence-specific single-stranded-DNA-binding properties of the encoded protein. Mol Cell Biol 12:5673–5682.

Cardoso MC, Leonhardt H, Nadal-Ginard B. 1993. Reversal of terminal differentiation and control of DNA replication: cyclin A and Cdk2 specifically localize at subnuclear sites of DNA replication. Cell 74:979–992.

Chang CF, Gallia GL, Muralidharan V, Chen NN, Zoltick P, Johnson E, Khalili K. 1996. Evidence that replication of human neurotropic JC virus DNA in glial cells is regulated by the sequence-specific single-stranded DNA-binding protein Pur alpha. J Virol 70:4150–4156.

Chepenik LG, Tretiakova AP, Krachmarov CP, Johnson EM, Khalili K. 1998. The single-stranded DNA binding protein, Pur-alpha, binds HIV-1 TAR RNA and activates HIV-1 transcription. Gene 210:37–44.

Danos O, Mulligan RC. 1988. Safe and efficient generation of recombinant retroviruses with amphotropic and ecotropic host ranges. Proc Natl Acad Sci USA85:6460–6464.

Dhar KK, Branigan K, Parkes J, Howells RE, Hand P, Musgrove C, Strange RC, Fryer AA, Redman CW, Hoban PR. 1999. Expression and subcellular localization of

cyclin D1 protein in epithelial ovarian tumour cells. Br J Cancer 81:1174–1181.

Diehl JA, Cheng M, Roussel MF, Sherr CJ. 1998. Glycogen synthase kinase-3beta regulates cyclin D1 proteolysis and subcellular localization. Genes Dev 12:3499–3511.

Ewen ME, Sluss HK, Sherr CJ, Matsushime H, Kato J, Livingston DM. 1993. Functional interactions of the retinoblastoma protein with mammalian D- type cyclins. Cell 73:487–497.

Fan J, Bertino JR. 1997. K-ras modulates the cell cycle via both positive and negative regulatory pathways. Oncogene 14:2595–2607.

Filmus J, Robles AI, Shi W, Wong MJ, Colombo LL, Conti CJ. 1994. Induction of cyclin D1 overexpression by activated ras. Oncogene 9:3627–3633.

Gallia GL, Darbinian N, Johnson EM, Khalili K. 1999. Self-association of Puralpha is mediated by RNA. J Cell Biochem 74:334–348.

Gallia GL, Johnson EM, Khalili K. 2000. SURVEY AND SUMMARY: Puralpha: a multifunctional single-stranded DNA- and RNA-binding protein [In Process Citation]. Nucleic Acids Res 28:3197–3205.

Haas S, Thatikunta P, Steplewski A, Johnson EM, Khalili K, Amini S. 1995. A 39-kD DNA-binding protein from mouse brain stimulates transcription of myelin basic protein gene in oligodendrocytic cells. J Cell Biol 130: 1171–1179.

Hagting A, Karlsson C, Clute P, Jackman M, Pines J. 1998. MPF localization is controlled by nuclear export. Embo J 17:4127–4138.

Herault Y, Chatelain G, Brun G, Michel D. 1992. V-src-induced-transcription of the avian clusterin gene. Nucleic Acids Res 20:6377–6383.

Herault Y, Chatelain G, Brun G, Michel D. 1995. RNA-dependent DNA binding activity of the Pur factor, potentially involved in DNA replication and gene transcription. Gene Exp 4:85–93.

Itoh H, Wortman MJ, Kanovsky M, Uson RR, Gordon RE, Alfano N, Johnson EM. 1998. Alterations in Pur alpha levels and intracellular localization in the CV-1 cell cycle. Cell Growth Diff 9:651–665.

Johnson EM, Chen PL, Krachmarov CP, Barr SM, Kanovsky M, Ma ZW, Lee WH. 1995. Association of human Pur alpha with the retinoblastoma protein, Rb, regulates binding to the single-stranded DNA Pur alpha recognition element. J Biol Chem 270:24352–24360.

Johnson EM, Karn J, Allfrey VG. 1974. Early nuclear events in the induction of lymphocyte proliferation by mitogens. Effects of concanavalin A on the phosphorylation and distribution of non-histone chromatin proteins. J Biol Chem 249:4990–4999.

Kang JS, Krauss RS. 1996. Ras induces anchorage-independent growth by subverting multiple adhesion-regulated cell cycle events. Mol Cell Biol 16:3370–3380.

Karn J, Johnson EM, Vidali G, Allfrey VG. 1974. Differential phosphorylation and turnover of nuclear acidic proteins during the cell cycle of synchronized HeLa cells. J Biol Chem 249:667–677.

Kato J, Matsushime H, Hiebert SW, Ewen ME, Sherr CJ. 1993. Direct binding of cyclin D to the retinoblastoma gene product (pRb) and pRb phosphorylation by the cyclin D-dependent kinase CDK4. Genes Dev 7:331–342.

Kawada M, Yamagoe S, Murakami Y, Suzuki K, Mizuno S, Uehara Y. 1997. Induction of p27Kip1 degradation and anchorage independence by Ras through the MAP kinase signaling pathway. Oncogene 15:629–637.

Kelm RJ, Jr, Elder PK, Getz MJ. 1999. The single-stranded DNA-binding proteins, puralpha, purbeta, and MSY1 specifically interact with an exon 3-derived mouse vascular smooth muscle alpha-actin messenger RNA sequence [In Process Citation]. J Biol Chem 274:38268–38275.

Kelm RJ, Jr, Elder PK, Strauch AR, Getz MJ. 1997. Sequence of cDNAs encoding components of vascular actin single-stranded DNA-binding factor 2 establish identity to Puralpha and Purbeta. J Biol Chem 272:26727–26733.

King RW, Glotzer M, Kirschner MW. 1996. Mutagenic analysis of the destruction signal of mitotic cyclins and structural characterization of ubiquitinated intermediates. Mol Biol Cell 7:1343–1357.

Kinoshita S, Chen BK, Kaneshima H, Nolan GP. 1998. Host control of HIV-1 parasitism in T cells by the nuclear factor of activated T cells. Cell 95:595–604.

Krachmarov CP, Chepenik LG, Barr-Vagell S, Khalili K, Johnson EM. 1996. Activation of the JC virus Tat-responsive transcriptional control element by association of the Tat protein of human immunodeficiency virus 1 with cellular protein Pur alpha [published erratum appears in Proc Natl Acad Sci USA 1997 Aug 19;94(17): 9571]. Proc Natl Acad Sci USA93:14112–14117.

Lasham A, Lindridge E, Rudert F, Onrust R, Watson J. 2000. Regulation of the human fas promoter by YB-1, Puralpha and AP-1 transcription factors. Gene 252:1–13.

Le Beau MM, Espinosa R, 3rd, Neuman WL, Stock W, Roulston D, Larson RA, Keinanen M, Westbrook CA. 1993. Cytogenetic and molecular delineation of the smallest commonly deleted region of chromosome 5 in malignant myeloid diseases. Proc Natl Acad Sci USA90: 5484–5488.

Lezon-Geyda K, Najfeld V, Johnson EM. 1997. The *PURA* gene, encoding the single-stranded-DNA-binding protein Pur. Alpha as a marker for 5q31 alteration in myeloproliferative disorders, a potential early step in induction of AML. FASEB 11:A100.

Li M, Strand D, Krehan A, Pyerin W, Heid H, Neumann B, Mechler BM. 1999. Casein kinase 2 binds and phosphorylates the nucleosome assembly protein-1 (NAP1) in Drosophila melanogaster. J Mol Biol 293:1067–1084.

Liu JJ, Chao JR, Jiang MC, Ng SY, Yen JJ, Yang-Yen HF. 1995. *Ras* transformation results in an elevated level of cyclin D1 and acceleration of G1 progression in NIH 3T3 cells. Mol Cell Biol 15:3654–3663.

Ma ZW, Pejovic T, Najfeld V, Ward DC, Johnson EM. 1995. Localization of *PURA*, the gene encoding the sequence-specific single- stranded-DNA-binding protein Pur alpha, to chromosome band 5q31. Cyto Cell Genet 71:64–67.

Morgenstern JP, Land H. 1990. A series of mammalian expression vectors and characterisation of their expression of a reporter gene in stably and transiently transfected cells. Nucleic Acids Res 18:1068.

Mulcahy LS, Smith MR, Stacey DW. 1985. Requirement for ras proto-oncogene function during serum-stimulated growth of NIH 3T3 cells. Nature 313:241–243.

Osugi T, Ding Y, Miki N. 1996a. Characterization of single-stranded cAMP response element binding protein (ssCRE-BP) from mouse cerebellum. Ann N Y Acad Sci 801:39–50.

Osugi T, Ding Y, Tanaka H, Kuo CH, Do E, Irie Y, Miki N. 1996b. Involvement of a single-stranded DNA binding protein, ssCRE-BP/Pur alpha, in morphine dependence. FEBS Lett 391:11–16.

Palmqvist R, Stenling R, Oberg A, Landberg G. 1998. Expression of cyclin D1 and retinoblastoma protein in colorectal cancer. Eur J Cancer 34:1575–1581.

Pear WS, Nolan GP, Scott ML, Baltimore D. 1993. Production of high-titer helper-free retroviruses by transient transfection. Proc Natl Acad Sci USA90: 8392–8396.

Pederson B, Jensen IM. 1991. Clinical and prognostic implications of chromosome 5q deletions: 96 high resolution studied patients. Leukemia 5:566–573.

Petersen BO, Wagener C, Marinoni F, Kramer ER, Melixetian M, Denchi EL, Gieffers C, Matteucci C, Peters JM, Helin K. 2000. Cell cycle- and cell growth-regulated proteolysis of mammalian CDC6 is dependent on APC-CDH1. Genes Dev 14:2330–2343.

Pfleger CM, Kirschner MW. 2000. The KEN box: an APC recognition signal distinct from the D box targeted by Cdh1. Genes Dev 14:655–665.

Pines J, Hunter T. 1991. Human cyclins A and B1 are differentially located in the cell and undergo cell cycle-dependent nuclear transport. J Cell Biol 115:1–17.

Piperno G, LeDizet M, Chang XJ. 1987. Microtubules containing acetylated alpha-tubulin in mammalian cells in culture. J Cell Biol 104:289–302.

Quelle DE, Ashmun RA, Shurtleff SA, Kato JY, Bar-Sagi D, Roussel MF, Sherr CJ. 1993. Overexpression of mouse D-type cyclins accelerates G1 phase in rodent fibroblasts. Genes Dev 7:1559–1571.

Rechsteiner M, Rogers SW. 1996. PEST sequences and regulation by proteolysis. Trends Biochem Sci 21:267–271.

Reddy JC, Hosono S, Licht JD. 1995. The transcriptional effect of WT1 is modulated by choice of expression vector. J Biol Chem 270:29976–29982.

Resnitzky D. 1997. Ectopic expression of cyclin D1 but not cyclin E induces anchorage-independent cell cycle progression. Mol Cell Biol 17:5640–5647.

Sherr CJ, Roberts JM. 1995. Inhibitors of mammalian G1 cyclin-dependent kinases. Genes Dev 9:1149–1163.

Spector DL, Smith HC. 1986. Redistribution of U-snRNPs during mitosis. Exp Cell Res 163:87–94.

Stacey DW, Hitomi M, Kanovsky M, Gan L, Johnson EM. 1999. Cell cycle arrest and morphological alterations following microinjection of NIH3T3 cells with Pur alpha. Oncogene 18:4254–4261.

Tretiakova A, Otte J, Croul SE, Kim JH, Johnson EM, Amini S, Khalili K. 1999. Association of JC virus large T antigen with myelin basic protein transcription factor (MEF-1/Puralpha) in hypomyelinated brains of mice transgenically expressing T antigen. J Virol 73:6076–6084.

Weinberg RA. 1995. The retinoblastoma protein and cell cycle control. Cell 81:323–330.

Winston JT, Coats SR, Wang YZ, Pledger WJ. 1996. Regulation of the cell cycle machinery by oncogenic ras. Oncogene 12:127–134.

Wortman MJ, Krachmarov CP, Kim JH, Gordon RG, Chepenik LG, Brady NN, Gallia GL, Khalili K, Johnson EM. 2000. Interaction of HIV- Tat with Pur-alpha in nuclei of human glial cells: characterization of RNA-mediated protein-protein binding. J Cell Biochem [in press]

Yang J, Bardes ES, Moore JD, Brennan J, Powers MA, Kornbluth S. 1998. Control of cyclin B1 localization through regulated binding of the nuclear export factor CRM1. Genes Dev 12:2131–2143.

Zambrano N, De Renzis S, Minopoli G, Faraonio R, Donini V, Scaloni A, Cimino F, Russo T. 1997. DNA-binding protein Pur alpha and transcription factor YY1 function as transcription activators of the neuron-specific FE65 gene promoter. Biochem J 328:293–300.